Los Alamos NATIONAL LABORATORY EST.1943

LA-UR-14-28568 (Accepted Manuscript)

The Seismic Noise Environment of Antarctica

Anthony, Robert E.
Rowe, Charlotte Anne
Aster, Richard C.
Wiens, Douglas
Nyblade, Andrew
Anandakrishnan, Sridhar
Winberry, J. Paul
Wilson, Terry

Provided by the author(s) and the Los Alamos National Laboratory (2015-12-09).

To be published in: Seismological Research Letters, Vol.86, iss.1, p.89-100, JAN-FEB 2015

DOI to publisher's version: 10.1785/0220140109

Permalink to record: http://permalink.lanl.gov/object/view?what=info:lanl-repo/lareport/LA-UR-14-28568

Disclaimer:
Approved for public release. Los Alamos National Laboratory, an affirmative action/equal opportunity employer, is operated by the Los Alamos National Security, LLC for the National Nuclear Security Administration of the U.S. Department of Energy under contract DE-AC52-06NA25396. Los Alamos National Laboratory strongly supports academic freedom and a researcher's right to publish; as an institution, however, the Laboratory does not endorse the viewpoint of a publication or guarantee its technical correctness.

RESEARCH LIBRARY

The Seismic Noise Environment of Antarctica

by Robert E. Anthony, Richard C. Aster, Douglas Wiens, Andrew Nyblade, Sridhar Anandakrishnan, Audrey Huerta, J. Paul Winberry, Terry Wilson, and Charlotte Rowe

Online Material: Table of station parameters; figures of mean acceleration power differences, interpolated noise maps.

INTRODUCTION

Seismographic coverage of Antarctica prior to 2007 consisted overwhelmingly of a handful of long running and sporadically deployed transient stations, many of which were principally collocated with scientific research stations. Despite very cold temperatures, sunless winters, challenging logistics, and extreme storms, recent developments in polar instrumentation driven by new scientific objectives have opened up the entirety of Antarctica to year-round and continuous seismological observation (e.g., Nyblade *et al.*, 2012).

Motivations for these recent studies include improved understanding of seismogenic, volcanic, tectonic and glaciological processes, heat flow, dynamic glaciological/ocean interactions, and mantle viscosity. Such studies contribute generally to improvements in understanding the geophysical, geological, and glaciological history of the continent and how these processes interact with the past and present state of the glaciological and climate system (e.g., Winberry *et al.*, 2009; Hansen *et al.*, 2010; West *et al.*, 2010; Winberry *et al.*, 2011; Heeszel *et al.*, 2013; Lough *et al.*, 2013; Chaput *et al.*, 2014; Accardo *et al.*, 2014), including processes relevant to glacial isostatic adjustment and sea level rise (Intergovernmental Panel on Climate Change [IPCC] Report, 2007). In addition, microseisms arising from ocean wave activity contain useful climate proxy information on the state and variability of the relatively poorly sensed southern oceans (Aster *et al.*, 2008; Stutzmann *et al.*, 2009; Aster *et al.*, 2010), and such observations are sensitive to sea ice concentration and areal coverage in the polar regions (Grob *et al.*, 2011; Tsai and McNamara, 2011; Koch *et al.*, 2013).

This characterization of the seismic noise environment of Antarctica, documentation of instrument performance, and comparisons of installation conditions (e.g., ice vaults vs. rock sites) is intended to facilitate optimization of future seismological deployments in such environments. We analyze data from a range of recent experiments to provide a broad geographical characterization of Antarctica's seismic noise environment, which can now include more substantial observations from regions that are free from anthropogenic noise contamination.

METHODS

Data Collection and Analysis

The Polar Earth Observing Network (POLENET ANET) and Gamburtsev Antarctic Mountains Seismic Experiment (GAMSEIS/AGAP; e.g., Heeszel *et al.*, 2013; Lloyd *et al.*, 2013; Wiens *et al.*, 2013; Chaput *et al.*, 2014) deployments of year-round temporary seismic stations have strongly contributed to improving the broadband seismic coverage of Antarctica (Fig. 1). Stations in POLENET ANET and GAMSEIS/AGAP were first deployed in December 2007 and have continued through the present. Although most stations were deployed in snow vaults, some sensors, particularly in the Transantarctic Mountains (TAMs) were installed directly on isolated rock outcrops, permitting some data quality comparisons to be performed between the two siting environments. All rock- and ice-sited temporary stations analyzed here were equipped with either Nanometrics Trillium 240 or Güralp cold-modified CMG-3T broadband sensors.

To characterize and analyze the seismic background of Antarctica, we examined all available 40 and 20 Hz sampling rate seismic data from 77 stations (Ⓔ Table S1, available in the electronic supplement to this article; 9 permanent sites, 38 POLENET, 30 AGAP) between 2007 and 2012 using data retrieved from Incorporated Research Institutions for Seismology (IRIS) Data Services. The seismic time series were then used to generate acceleration power spectral densities (PSDs; in dB relative to 1 $m^2/s^4/Hz$) and PSD probability density functions (PDFs) using the methodology of McNamara and Buland (2004) through the software package PQLX (McNamara and Boaz, 2011; Fig. 2). The PSD estimation procedure deconvolves the instrument response from archived continuous time series. One-hour, 50% overlapping time segments are windowed into 13 subsegments with 75% overlap. Each subsegment is demeaned and detrended, and a 10% cosine taper is applied to reduce spectral leakage. Welch's section averaging method is utilized to estimate the PSD (e.g., Oppenheim and Schafer, 1975) for each 1 hr segment using the 13 subsegments. Empirical PDFs are constructed by binning periods in 1/8-octave intervals and power in 1 dB intervals, and normalizing by the total number of PSDs. PSD PDFs and other statistics are referenced to the Peterson (1993) global new high- and

doi: 10.1785/0220140109

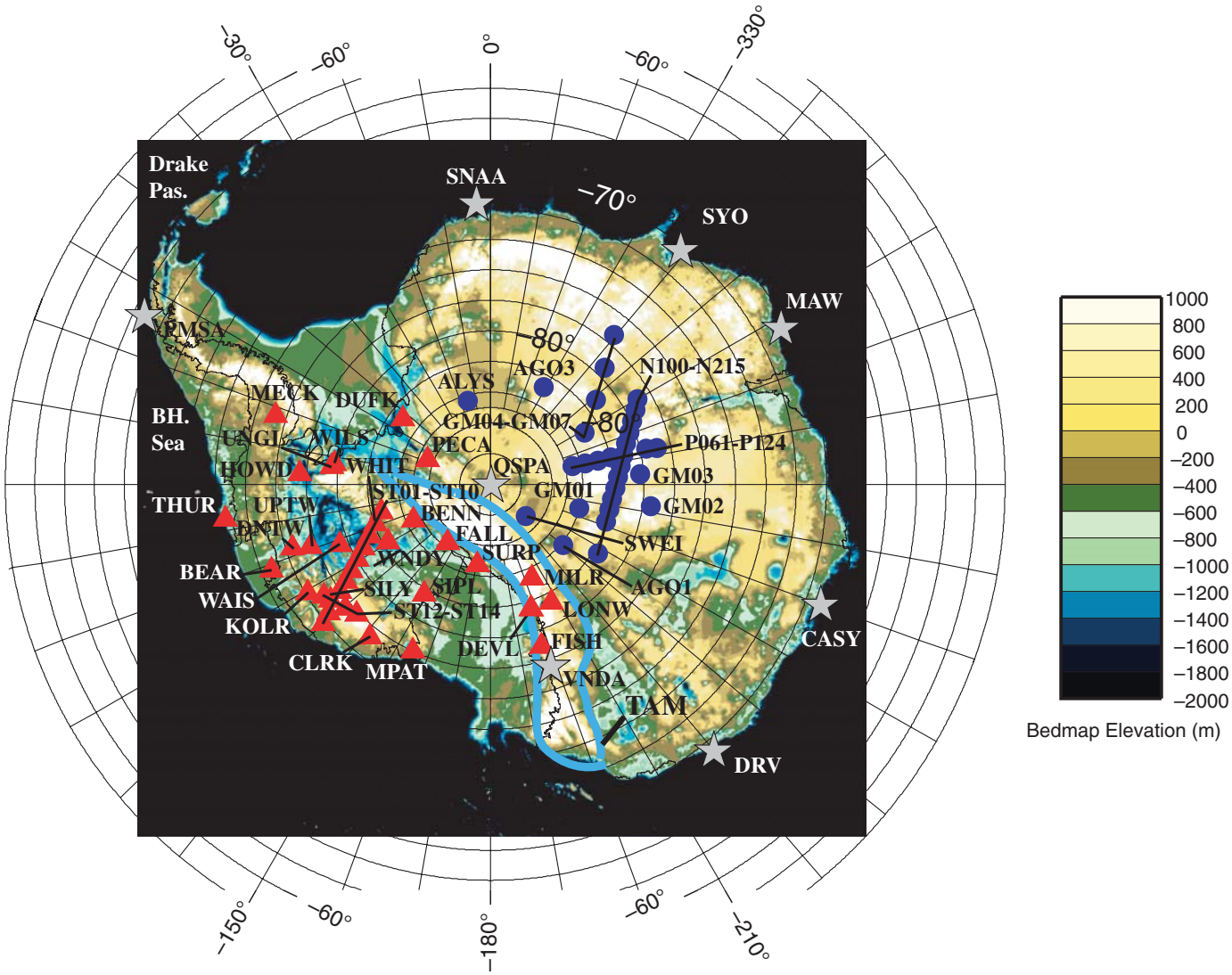

▲ **Figure 1.** The Polar Earth Observing Network (red triangles) and Gamburtsev Antarctic Mountains Seismic Experiment (GAMSEIS/AGAP; blue circles) year-round seismic stations deployed since 2007. Prior to 2007, coverage was substantially limited to longer-operating stations sited near scientific bases (gray stars) and confined to the coast (with the exception of South Pole; QSPA). The Transantarctic Mountains (TAM) are outlined in blue and the Bellingshausen Sea (BH. Sea) and Drake Passage (Drake Pas.) are noted near the Antarctic Penninsula.

low-noise models (NHNM, NLNM) for broader global comparison.

PSD PDFs are insightful and compact data representations for examining instrumentation and data quality as well as seismic signals and noise levels. To identify background noise conditions, the PSD population was culled of obvious instrumentation artifacts associated with downtime and malfunctions. This was achieved, when necessary, by automatically identifying characteristically anomalous PSDs that contained power levels within the robust secondary microseism band that exceeded the 98th percentile statistics in every period bin or that fell below median NLNM power in at least 50% or the period bins. Such PSDs were attributed to common instrumentation artifacts such as mass recenters, calibrations (e.g., McNamara and Buland, 2004), and to intermittent data dropouts due to power or other issues. The number of resulting PSDs relative to the station installation time was then used to assess each station's uptime. Stations exhibiting less than 50% uptime and/or failing to record at least one cycle of a seasonally representative one month or longer time segment were excluded from our noise maps but were included in the analyses of instrumentation performance. PSDs that were strongly affected by earthquake signals do not require special consideration because they are sufficiently intermittent that they do not significantly affect the median or other central PSD PDF metrics calculated here (e.g., Aster *et al.*, 2008, 2010). For the instrumentation used in this study, the nominal digitizer/seismometer electromechanical noise level is generally substantially below the seismic noise field (e.g., Peterson, 1993; Wilson *et al.*, 2002; Ringler and Hutt, 2010) and thus usually do not

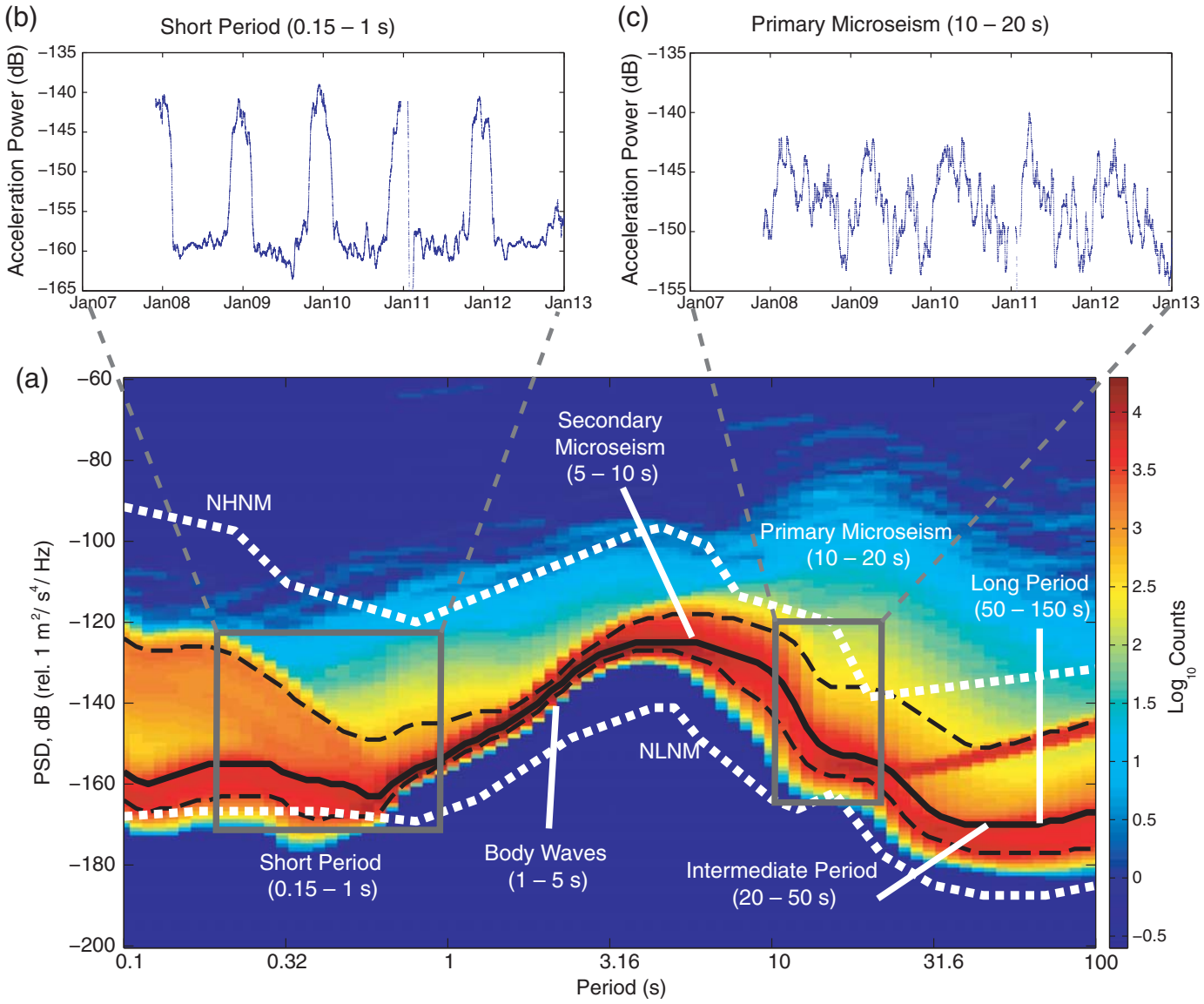

▲ **Figure 2.** (a) The probability density function of power spectral density (PSD) for the vertical-component of South Pole station QSPA (146 m borehole) for December 2007–December 2012 plotted on a logarithmic color scale to show transient high-amplitude signals (e.g., teleseismic earthquakes) and other probabilistically secondary features. The median PSD is plotted (solid black line) as well as 5th and 95th percentile statistics (dashed lines) and are compared to the global high- and low-noise models of Peterson (1993). In addition, the six period bands referred to in the text are labeled. (b) Temporal evolutions in power in the short period and (c) primary microseism band are shown to illustrate the influence of seasonal anthropogenic noise at nearby (7.8 km) Amundsen–Scott South Pole Station and the unique seasonality (phase shifted ~90° from the rest of the southern hemisphere; Aster *et al.*, 2008) of the Antarctic microseism signal due to the annual growth and decay of sea ice.

affect these metrics (the exception being at extremely quiet sites such as ice boreholes at short period [<0.1 s]).

Noise Band Characterization

To evaluate the spatial distribution of the seismic noise state at these stations, we separated the median PSD of each station component into six period bands (Fig. 2) of interest to source and imaging seismology and examined the median power in each.

The short-period band, 0.15–1.0 s, captures common sources of anthropogenic noise, seismic coupling due to wind (e.g., Li *et al.*, 1984; Galperin *et al.*, 1986; Peterson, 1993; Withers *et al.*, 1996; Young *et al.*, 1996), as well as signals ranging from local glaciological movements to teleseismic earthquakes.

The 1.0–5.0 s teleseismic body waveband is shared by intermittently excited local, regional, and teleseismic earthquake-generated body waves, which are key to structural and source-related studies. In addition, several recent studies have attributed

noise in this band at near-coastal and near-lake stations to local or regional swell activity (Bromirski *et al.*, 2005; Tsai and McNamara, 2011; Aleqabi *et al.*, 2013), which constitutes the shorter period portion of the double-frequency (secondary) microseism.

The 5.0–10.0 s and 10.0–20.0 s secondary and primary microseism bands, respectively, are dominated, in the absence of earthquake or other transient source excitation, by ocean-generated Rayleigh waves. The primary microseism originates when deep-ocean waves break or shoal on a shallow seafloor and are primarily converted into Rayleigh waves (e.g., Hasselmann, 1963). The typically much more powerful secondary microseism is usually generated by standing-wave components of the oceanic wavefield (e.g., coastal reflections, storm–storm, or intrastorm wave interactions; Ardhuin *et al.*, 2011) that generate seafloor forcing at half the period of the constituent traveling ocean waves (e.g., Longuet-Higgins, 1950; Tanimoto, 2007). Variations in microseism power at specific stations in Antarctica are known to be strongly sensitive to both near-coastal storms and to wave state (e.g., MacAyeal *et al.*, 2006) and are amplitude modulated by the annual formation and breakup of sea ice (Aster *et al.*, 2008, 2010; Grob *et al.*, 2011).

The 20–50 s intermediate period band contains power from the longest period microseisms and is strongly excited by intermediate-period surface waves from global earthquakes.

The 50–150 s long period band is controlled by low-amplitude (e.g., ~300 time smaller in power than double-frequency microseism excitation) oceanic excitation of long-period waves generated through infragravity wave excitation and difference–frequency interaction of opposing ocean wavetrains (Rhie and Romanowicz, 2004; Traer *et al.*, 2012). A common source of instrumentally generated noise in this band is diurnal or other seismometer tilting that strongly couples into the horizontal components (e.g., Sorrells, 1971; Peterson, 1993; Wilson *et al.*, 2002). This period band is also intermittently excited by long-period teleseismic surface waves from large earthquakes.

RESULTS AND DISCUSSION

Polar Instrument Performance for Different Siting Methodologies

To evaluate the absolute and relative performance of year-round seismographs in Antarctica under different siting conditions, we cull the PSD dataset of obvious instrumentation artifacts as described previously and intercompare median PSD metrics (Fig. 3). Postartifact uptimes for different emplacement types were highly variable, with permanent stations (9) recording acceptable quality data 89% ± 3% of the time, POLENET ANET sites (38) at 83% ± 5%, and GAMSEIS/AGAP sites (30) at 66% ± 4%. The lower data retrieval rate of the AGAP sites reflects the extremely cold temperatures and consequent service and technical issues of working on the high elevation East Antarctic Plateau (annual average ambient temperatures of −50°C to −60°C and much colder temperatures during the winter). Subdividing the POLENET ANET sites into emplacement type shows an uptime advantage of ice sheet (91% ± 4%)

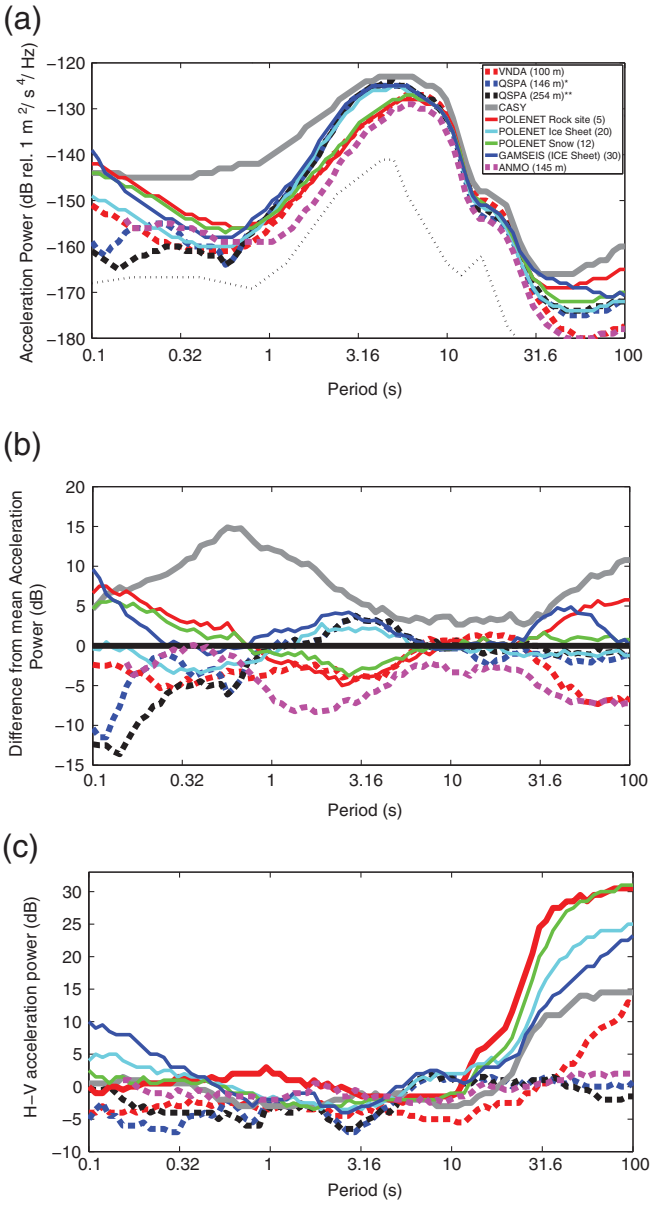

▲ **Figure 3.** (a) Median vertical-component PSDs for different siting types, as defined in the text, between 2008 and 2012 with the estimated Global Seismic Network low-noise models (light gray dashed line; Peterson, 1993). Borehole sensors are indicated by dashed lines, and the numbers in the legend represent the number of stations included in the median estimate or borehole depth. Because of intermittent instrumentation issues, we only used data from February 2011 to December 2012 for characterizing the 146 m QSPA borehole and omitted 2012 data for the 254 m borehole. For comparison to a high-quality North American site, we also show ANMO, which is a long-running GSN rock borehole located near Albuquerque, New Mexico (U.S.A.). (b) Removing the mean value of the PSD estimates in (a) displays relative noise level differences. (c) Subtracting the median horizontal power (attained from averaging the BHE (east–west) and BHN (north–south) PSDs) from vertical power for the different emplacement types shows substantial amplification of horizontal power at several sites, which are primarily attributable to tilt-coupled horizontal noise.

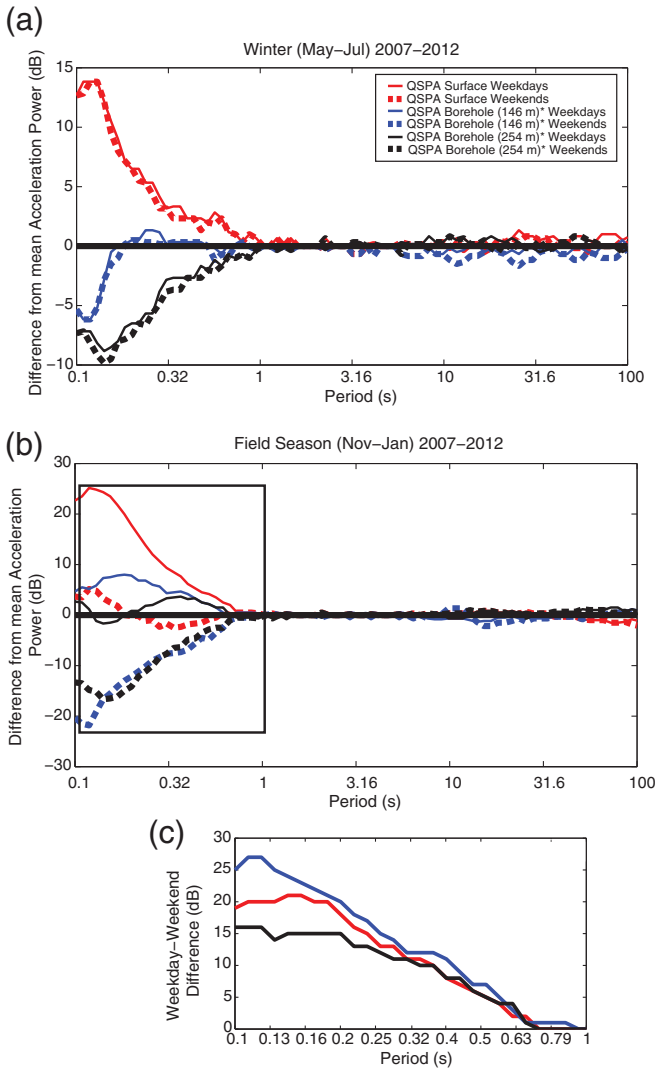

▲ **Figure 4.** Deviations of weekday (solid lines) and weekend (dashed lines) median vertical-component PSDs for the three sensor depths at the SPRESO site, incorporated into station QSPA, between 2007 and 2012 during (a) the winter (May–July) and (b) the field season (November–January). (c) Weekday/weekend differences for the boxed region in (b) shows the influence of anthropogenic noise from nearby (7.8 km) Amundsen–Scott South Pole Station during the field season. The 146 m borehole is the least effective at mitigating this cultural noise likely because it is located within the near-surface (~200 m) firn waveguide that traps high-frequency energy (Albert, 1998).

and shallow snow (84% ± 8%) siting scenarios compared to rock outcrops (72% ± 14%).

Median vertical-component PSDs for the limited number of available long-term stations and installation types reveal several intriguing differences (Fig. 3a,b). Unsurprisingly, the two borehole emplacements (VNDA, QSPA) are up to 20 dB quieter at high frequencies compared to surface sites, reflecting the effective mitigation of wind noise (e.g., Withers *et al.*, 1996). Rock and shallow snow POLENET ANET sites comprise the noisiest temporary seismic installations in the short-period band, being 5–7 dB noisier than comparable ice sheet sites. This is likely explained as (1) many of these stations are located in the TAMs, which is one of the windiest places on the continent (e.g., Mayewski *et al.*, 2009), and (2) these sites are located on/near rock outcrop topography that facilitates the coupling of wind energy into seismic noise. In addition, stations placed directly on rock outcrops show enhanced horizontal noise, which we interpret as tilt, at periods of 0.5–3 s, as evidenced by a 5 dB difference between horizontal- and vertical-component noise (Fig. 3c). We hypothesize that this is also a result of wind forcing on the exposed outcrop and instrumentation enclosure. It should be noted that even these noisy POLENET ANET sites in the TAMs are characteristically 10–15 dB quieter in the short-period band than permanent base-sited coastal stations at CASY, PMSA, DRV, which are affected by persistent circumpolar westerly winds and probably also all have some significant level of anthropogenic noise for part of the year (Figs. 3 and 5). Between 0.3 and 2 s, these coastal, permanent pier and vault stations are the noisiest population by 3–15 dB and have a distinct peak in noise at ~0.5 s relative to other stations, suggestive of the buildings or other structures around the station being excited by the wind in this period band (Ⓔ Fig. S1).

The teleseismic body waveband reveals that the noise levels observed between rock and ice sites diverges between 1.25 and 7 s period, with ice site median levels being ~9 dB noisier at 3 s (Fig. 3b). The noise in this band is comprised mainly of Rayleigh waves generated by near-coastal primary and secondary microseism sources. Using experimentally determined seismic velocities in ice sheets beneath the firn-ice transition (V_P = 3.8 km/s; e.g., Kohnen, 1974; Albert, 1998) compared to a fast (6.2 km/s) upper crust for a bedrock site yields a local amplification of ~2.5 dB. Thus, this phenomenon cannot be entirely attributed to the simple elastic seismic-wave amplitude effects of the ice sheet and could be the result of an exceptionally strong contribution from the shallower snow, including that above the firn-ice transition (V_P = ~0.5–3 km/s; Albert, 1998) and/or to trapped energy in the ice-sheet-atop-bedrock waveguide near these periods. We additionally note an ~4.5 dB increase in the difference between horizontal- and vertical-component noise (Fig. 3c) throughout this amplified secondary microseism band at ice sites relative to rock sites, which may reflect the influence of a smaller Poisson's ratio (i.e., $\sigma \sim 0.2$) in the upper ice sheet relative to rock sites.

Noise levels are relatively consistent in the primary and secondary microseism bands for all installation types with the exception of the near coastal site CASY. The intermediate period band between 20 and 50 s has ~5 dB of elevated noise on the AGAP stations. Closer examination of these stations revealed a newly recognized source of instrument noise that was ultimately linked to the formation of convection cells within the sensor due to sensor heat dissipation under extremely cold ambient temperature conditions (Anthony *et al.*, 2011; T. Parker (Incorporated Research Institutions for Seismology [IRIS] Program for the Array Seismic Studies of the

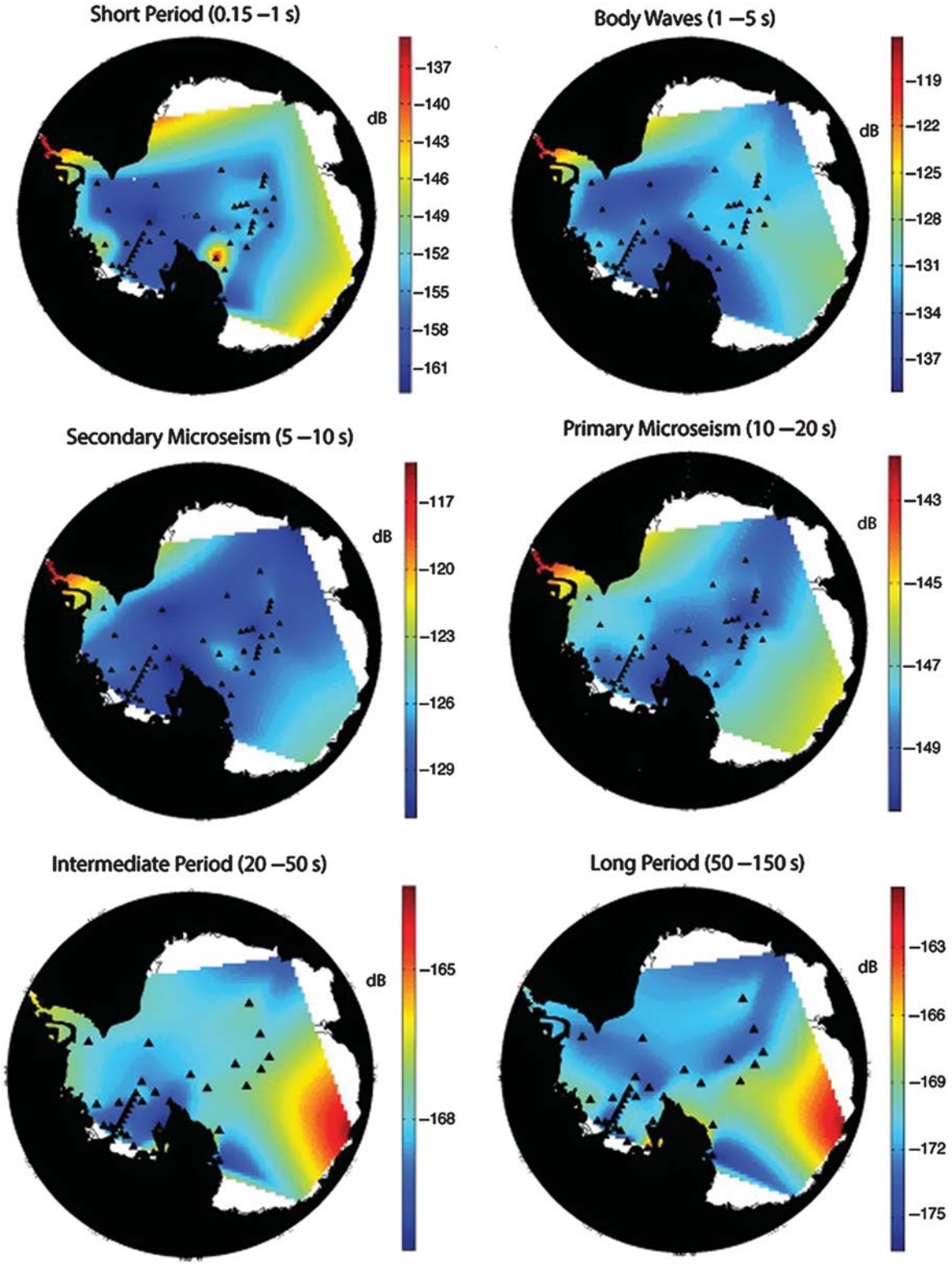

▲ **Figure 5.** Interpolated noise-map of Antarctica for each of six separate period bands (Fig. 2) using median vertical-component power in each for 59 seismic stations (QSPA surface station used) located across the continent (triangles). Color scale changes with each period range to illustrate contrast and represents acceleration power in decibels. MILR is the red dot in the TAMs in the short-period map and reflects the exceptional wind coupling at this unstable rock site. Long-period sensor tilt at MILR is severe, and the station has been omitted from the intermediate- and long-period maps. Stations afflicted with the long-period convection noise (HOWD, several GAMSEIS/AGAP sites) were also omitted from these two frequency bands. The large red feature in East Antarctica is controlled by one very noisy coastal station (CASY; Fig. 3).

Continental Lithosphere [PASSCAL], personal comm., 2012). This phenomenon produces noise at periods of ~30–70 s and only affects the vertical components of a few sensors, mostly those located on the East Antarctic Plateau (Ⓔ Fig. S2), and is generally absent during the warmer summer months.

A Case Study of QSPA (South Pole): Implications for Icecap Borehole Sensors

Borehole installations at tens to hundreds of meters substantially reduce wind noise as well as some types of anthropogenic noise (e.g., Young *et al.*, 1996; McNamara and Buland, 2004). QSPA is a unique installation that incorporates borehole sensors installed within the nearly 3000 m thick south polar icecap. It is the only such station in the Global Seismographic Network, which includes a large number of conventional bedrock borehole sites (Butler *et al.*, 2004). The QSPA site is a component of the South Pole Remote Earth Science and Seismological Observatory (SPRESO), sited 7.9 km from the Pole and the Amundsen–Scott (US) South Pole Station within a designated vibrational Quiet Sector for South Pole science operations. The transition from snow to compact ice as a result of pressure with increasing depth results in a laterally uniform seismic velocity gradient within the upper 200 m of the ice sheet (Gow, 1963, 1975; Patterson, 1994). Modeling of short-period anthropogenic noise within this velocity model indicates that surface-generated noise is trapped in the near-surface firn layer (Albert, 1998). Two of the three QSPA borehole sensors were installed below 200 m to be located beneath this waveguide.

The multiple seismic instruments collocated at QSPA provide an opportunity to compare the noise levels of surface vault seismometers with borehole instruments in a continental interior ice sheet environment. Recording at QSPA began in January of 2003, where three borehole instruments (at 275, 254, and 146 m) were supplemented with additional sensors located in vaults 4 m below the surface. The station received numerous sensor replacements and updates during its development and testing between 2009 and 2011 (K. Anderson and T. Storm, personal comm., 2013). Here, we analyze data from longer contiguous periods of the archive collected at the surface vault and with borehole Güralp CMG3-T sensors at 146 m after February 2011 and at 254 m between 2007 and 2011.

Overall, baseline (winter), high-frequency (5–10 Hz) noise power is lower by 15–25 dB in the borehole installations on all components. This advantage diminishes with increasing period until ~1 s, beyond which noise levels for the surface and borehole sites are nearly identical (Fig. 4a). The 254 m deep borehole is several dB quieter than the sensor at a depth of 146 m at frequencies greater than 1 Hz, with the greatest improvement of ~5 dB observed between frequencies of 3–5 Hz. Noise levels during the weekend and during the weekday are similar during austral winter months of highly reduced human activity (February–October), suggesting that the natural background noise state, free from anthropogenic contamination, is approached at the SPRESO site during this part of the year. The vertical-component noise is nearly uniform between the surface and borehole sites at long periods, but the horizontal components of the borehole sensors are 35–40 dB quieter than the surface at 100 s, due to the strongly reduced tilting of these clamped sensor packages relative to shallow ice vaults (Fig. 3c). This reduction in long-period, horizontal-component noise is 10 dB greater than that noted between rock boreholes and nearby surface vaults in the southwestern United States (Wilson *et al.*, 2002).

During the austral summer (November–January), there is a large difference between the weekday noise and the weekend noise levels (up to 26 dB), in the high-frequency band (< 1 s) showing that anthropogenic noise from the South Pole station is readily detected at all depths (Fig. 4b). Subtracting weekend from weekday power levels (Fig. 4c), we observe that station activities at the South Pole during the busiest season at the base results in a 15–25 dB increase in high-frequency (0.1–0.2 s) noise that decays approximately exponentially with increasing period. A likely significant source of this noise is the frequent grooming of the snow runways by heavy equipment (Anderson *et al.*, 2008). The 254 m deep borehole sensor, located well below the firn–ice transition (van den Broeke, 2008), is seen to be most effective at mitigating anthropogenic noise by up to ~5 dB compared to the surface vault and by up to ~10 dB compared to the 146 m borehole, which lies within the (upper ~200 m). These results thus support the Albert (1998) model prediction that high-frequency seismic energy from surface sources is substantially trapped in the shallow Antarctic icecap.

The Continent-Scale Seismic Noise Environment of Antarctica

To produce estimates of median vertical-component noise level variations across the continent (recognizing that the spatial sampling is of course still very sparse), power levels in the above-defined period bands at each station were geographically interpolated on an equal area, UTM-style, mesh grid (Fig. 5; Ⓔ horizontal-component noise level maps show similar trends see Figs. S3 and S4). A striking feature on these maps are the anomalously high and broadband (0.15–20 s), (5–20 dB) noise levels of the Antarctic Peninsula relative to the rest of the continent, with the discrepancy becoming stronger at shorter periods. This is likely primarily due to the high winds associated with the circumpolar westerlies and the resulting effects of tempestuous seas in the Drake Passage and Bellingshausen Sea, accentuated by the narrowness of the peninsula and station proximities to the coast.

Noise in the short-period band is also relatively high (~10 dB above the majority of the continental interior) at non-Peninsular coastal and central TAM sites. This is consistent with estimates of higher wind speeds in these areas from long-term (e.g., 40-year) weather reanalysis, for the central TAM and East Antarctic Coast (Mayewski *et al.*, 2009). Away from the Antarctic Peninsula and its exceptionally strong and broadband oceanic microseism noise, PSD median levels in the teleseismic body waveband (1–5 s) become much more uniform, varying by just ~7 dB, with the highest levels recorded at near-coastal stations and for sensors sited atop thick ice

sheets (e.g., GAMSEIS/AGAP; POLENET ANET Transect Stations; WAIS).

Generally, power in the primary and secondary microseism bands are highest at near-coastal stations and decay into the continental interior by up to 6 dB and 12 dB, respectively. The gradient of decay is period correlated and is most readily observable around the Antarctic Peninsula. Compared to most of the planet, noise levels in the entire microseism band (1–20 s) in Antarctic are strongly affected by the annual growth and decay of sea ice around the continent (Fig. 6; primary microseism shown for reference). In both microseism bands, seasonal power varies by at least 10 dB, with annual maxima occurring across most of the continent during the sea ice minimum, which occurs approximately three months prior to peak oceanic storm activity in the southern hemisphere (Aster *et al.*, 2008). Minimum noise in the microseism bands occurs during the summer across the continent, with the notable exception of primary microseism power at DRV. We suspect that high levels of local sea-ice loss early in the melt season may drive this phenomenon by exposing the Wilkes Land regional coastline and shelf to Southern Ocean waves earlier in the year. Previous analysis of microseism noise at DRV has shown that the primary microseism source back-azimuth shifts seasonally toward the closest ice-free ocean (Stutzmann *et al.*, 2009).

Comparing the noise environment of the Antarctic continent to long-running sites in interior North America allows for a simple comparison between these Antarctic noise levels and typical data recorded in the northern hemisphere (e.g., by EarthScope USArray). We compared the median PSD metrics calculated in this study (Fig. 3) to a 145 m rock borehole sensor at GSN station ANMO (Albuquerque, New Mexico, U.S.A.). In general, Antarctic stations are ∼5 dB quieter at short periods (< 1 s) than ANMO, likely because of limited anthropogenic noise contributions, greatly reduced wind profiles, and potentially poorly characterized short-period response at the 145 m ANMO borehole (Adam Ringler [USGS Albuquerque Seismic Laboratory], personal comm., 2014). However, even without considering the ice-sheet amplification effect widely observed between ∼1.25 and 7 s, West Antarctica is typically 2–5 dB noisier than ANMO in the microseism bands (1–20 s) despite being seasonally surrounded by a sea ice buffer. This likely reflects the more extreme wave states and storm activity present in the Southern Ocean relative to the northern Pacific Ocean, which dominates the microseism band at ANMO (e.g., Aster *et al.*, 2008).

CONCLUSIONS

Broadband seismic background noise for Antarctica is characterized using recently collected year-round data that have greatly expanded coverage across the continent. We analyzed noise levels within six discrete bands that encompass diverse sources of natural, anthropogenic, and instrument (e.g., tilt-coupled) noise and have broadly characterized the large-scale geographic distribution of power in each band across the continent and nominal noise level expectations for future Antarctic stations. We conclude the following regarding the various types of installations presently available for analysis.

Ice Borehole Stations

Despite detectable short-period-dominated anthropogenic noise during the busiest part of the year from the 7.8 km distant Amundsen–Scott South Pole Station, the borehole seismometers at QSPA are the quietest sensors in Antarctica at high frequencies (>∼2 Hz), occasionally dropping below the Peterson (1993) low-noise model, and are thus candidates for the quietest stations on earth in this frequency range. Our observations confirm that placing the sensor below the near-surface waveguide modeled by Albert (1998) (>∼200 m) results in an ∼5 dB reduction in baseline natural high-frequency noise and a 10 dB reduction in anthropogenic noise compared to a sensor located within the waveguide. In addition, the QSPA borehole instruments are the only ice-sited sensors in Antarctica to exhibit extremely low tilt-coupled horizontal-component noise at long periods (i.e., > 50 s) and attendant low general long-period noise levels. QSPA does experience an up to ∼9 dB amplification in background noise at 2–5 s similar to that observed on all thick ice sites, and that we conclude is a combination lowered seismic impedance and ice-atop-bedrock waveguide effect.

Rock Borehole Stations

The 100 m rock borehole VNDA, located in the McMurdo Dry Valleys, does not exhibit the amplified 2–5 s noise levels of QSPA and other ice sheet sites and is also ∼5 dB quieter than the QSPA boreholes and POLENET ANET ice vaults at 50–100 s, making it the quietest long-period instrument in Antarctica. The instrument does appear to exhibit some tilt-coupled noise at > 30 s period, as is visible in vertical/horizontal power ratios, but this discrepancy between components is smaller than for any other sensor on the continent except the QSPA ice borehole sensors. Short-period (< 1 s) noise levels at VNDA are better than any other Antarctic station, except for the QSPA boreholes, despite its location in the windy Dry Valleys and at the foot of the TAMs. This station is generally ∼10 dB quieter than comparable POLENET ANET rock sites; however, 8–30 s microseism power levels are 1–2 dB higher than typical stations in Antarctica, which we attribute to relative proximity to coastal microseism sources.

Together, the two borehole stations are the quietest sites in Antarctica between 0.15 and 100 s and are exceptionally impervious to wind and tilt-coupled horizontal noise. Because of their low long-period noise, establishing additional boreholes sites in Antarctica would significantly improve the ability to detect and study long-period signal generated by the cryospheric and tectonic processes in Antarctica. For instance, these two sites were the only stations capable of clearly detecting the 25–83 s slip signal generated by slow cryospheric events from the Whillans Ice Stream in West Antarctica by Wiens *et al.* (2008).

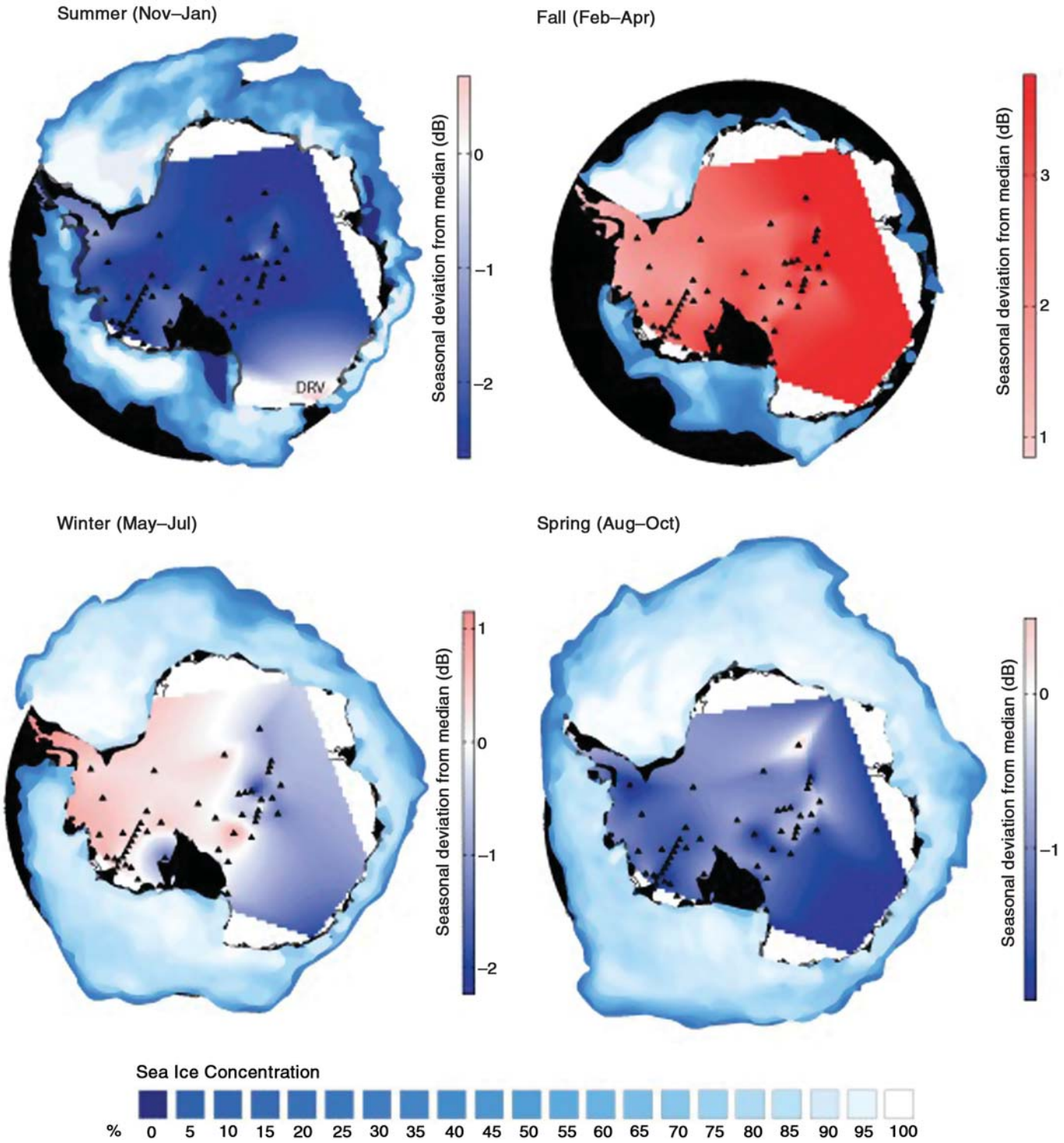

▲ **Figure 6.** Interpolated map of seasonal median differences from year-round medians in the primary microseism band (10–20 s) overlain on representative sea ice concentration maps from the middle month of each season during 2009 (Fetterer *et al.*, 2002). Red indicates station-interpolated regions that are noisier for a particular season than the median, and blue indicates regions that are quieter. Seasonal power variations in this band are strongly influenced by the annual build up and decay of sea ice, with the entire continent experiencing highest noise levels during the fall sea ice minimum. Nearly all of West Antarctica experiences above-average noise levels during the winter, likely in response to Southern Ocean swell interacting with the ice-free northern Antarctic Peninsula (Koch *et al.*, 2013). The Wilkes Land coastal region near Dumont d'Urville (DRV) is one of the earliest sections of Antarctic coastline to be directly exposed to Southern Ocean swell during early summer and consequently is the only area of the continent in this study to show above-average primary microseism power during this season.

Ice Sheet Stations

In general, POLENET ANET vaults, where sensors were typically deployed 1–2 m below the surface and atop thick ice sheets, were 5–7 dB quieter in the short-period band than comparable rock and near-rock/shallow snow vaults. These lower noise levels are partially attributable to the stations being deployed in less windy areas with flatter topography and accordingly lower levels of seismic wind coupling. In addition, many of these sites become covered drift, resulting in very low wind profiles. These sites are also 5–7 dB quieter at 30–100 s than rock/shallow snow vaults, reaching vertical noise levels that can approach the 254 m QSPA borehole in this band. GAMSEIS/AGAP ice vaults deployed on the East Antarctic Plateau experienced greater difficulty operating continuously in the exceptionally harsh East Antarctic environment. Some of these stations experienced strong, ~30–70 s, internal convection noise on the vertical components, a newly recognized process of internal seismometer noise generation that is now understood and being ameliorated (T. Parker, personal comm., 2012).

Rock and Shallow Snow Stations

Rock and shallow snow stations are here classified as those sited on top of and adjacent to isolated Nunataks and/or in close vicinity to TAM outcrops. In these locations, we found that emplacement in even shallow snow/ice was broadly superior to direct rock installation, particularly in improving long-period (> 10 s) sensor horizontal noise attributed to tilt, and in the near-elimination of shorter period tilt, which we suspect arises from direct wind forcing on the outcrop and station. At an especially noisy rock vault from POLENET ANET (MILR, Fig. 6), these wind-driven effects were so severe that the microseism peaks were sometimes obscured on PSD PDFs of the horizontal components and the station was rendered unusable for shear-wave splitting studies (Accardo *et al.*, 2014). In addition, we note that station uptimes for rock vaults (72%) are not as good as shallow-snow or ice vaults (84%, vs. 91%), primarily because these sites are more susceptible to damage from extreme storm events. In the future, we recommend installing stations that are near outcrops on adjacent snow rather than rock when possible.

Long-Term Stations with Bedrock Piers/Vaults

The longest operational seismographic stations in Antarctica, aside from the heterogeneous installations over the years at South Pole are collocated with coastal research stations and are consequently subject to anthropogenic, wind, and microseism noise. Between 0.3 and 2 s, these stations as a group are the noisiest in Antarctica. Compared to remote, temporary shallow snow vaults, the main seismic noise advantage of these installations, which incorporate larger-scale permanent piers, is convenience and reduced sensor tilt (i.e., an ~10 dB smaller discrepancy in H/V ratios at 100 s).

Using the long running GSN borehole station ANMO as an example of a long-running, high-quality station for reference, we find that many interior stations in Antarctica are quieter than ANMO at short periods (< 1 s) but also show more energy in the microseism bands (1–20 s) due to the content being surrounded by the Southern Ocean and despite lower noise levels arising from annual sea ice growth. Aside from the aforementioned ice-sheet-associated amplification between ~1.25 and 7 s, noise levels in Antarctica in the microseism-spanning bands are controlled by proximity to strong microseism source generation regions (especially the Antarctic Peninsula), and to seasonal and longer-term changes in southern ocean wave state and sea ice extent. Geographic variations in microseism power become less pronounced, but are still resolvable, at longer periods. Maximum power in these period bands generally occurs across the continent during the Austral fall, when annual ocean wave activity is increasing and sea ice coverage is at a minimum. The formation of the sea ice buffer during the winter slightly reduces yearly variations of microseism power in Antarctica (~10–15 dB) compared to nonpolar stations (e.g., 12–18 dB at ANMO).

Recent year-round seismic deployments in the remote interior of Antarctica have dramatically increased the quality and quantity of broadband data from large hitherto unsampled areas of the continent. These data are helping to drive significant new understanding about solid Earth, and glacial structures and processes (e.g., Lough *et al.*, 2013; Accardo *et al.*, 2014; Chaput *et al.*, 2014; Peng *et al.*, 2014). Uptimes of temporary ice-sheet vaults utilized in the POLENET ANET deployment rival those of many long-term stations collocated with research bases, yet show substantially reduced noise levels in the period bands of local and teleseismic earthquakes and ice quakes. These results indicate that the seismological community is now capable of both interrogating additional sections of polar and other cold regions and able to move toward the establishment of more geographically extensive and long-term Antarctic and Arctic seismographic networks.

ACKNOWLEDGMENTS

We express thanks to Tim Parker (Incorporated Research Institutions for Seismology–Program for the Array Seismic Studies of the Continental Lithosphere [IRIS-PASSCAL] Instrument Center), Kent Anderson (IRIS), Adam Ringler (U.S. Geological Survey [USGS] Albuquerque Seismological Laboratory), Dan McNamara (USGS, National Earthquake Information Center), and Susan Bilek and David Reusch (New Mexico Tech) for useful exchanges. The facilities of the IRIS Data Management System, and specifically the IRIS Data Management Center, were used for access to waveform and metadata required in this study. Sea ice concentration data around Antarctica were obtained from The National Snow and Ice Data Center (NSIDC). The Global Seismographic Network (GSN) is a cooperative scientific facility operated jointly by the IRIS, the USGS, and the National Science Foundation (NSF). The facilities of the IRIS Consortium are supported by the NSF under Cooperative Agreement EAR-1063471, NSF Polar Programs, and the Department of Energy National Nuclear Security Administration. POLENET-

Antarctica phase 1 was supported by NSF Polar Programs Grant Numbers 0632230, 0632239, 0652322, 0632335, 0632136, 0632209, and 0632185, and POLENET-Antarctica phase 2 is supported by NSF Polar Programs Grant Numbers 1246776, 1246712, and 1419268. Additional funding was provided by Los Alamos National Laboratory through the Institute of Geophysics, Planetary Physics. Additional information regarding the POLENET project, data collection sites, and geophysical data is available at polenet.org (last accessed October 2014).

REFERENCES

Accardo, N., D. Wiens, S. Hernandez, R. Aster, A. Nyblade, A. Huerta, S. Anandakrishnan, T. Wilson, and D. Heeszel (2014). Upper mantle seismic anisotropy beneath the West Antarctic Rift System and surrounding region from shear wave splitting analysis, *Geophys. J. Int.* **198,** 414–429.

Albert, D. G. (1998). Theoretical modeling of seismic noise propagation in firn at the South Pole, Antarctica, *Geophys. Res. Lett.* **25,** doi: 10.1029/1998GL900155.

Aleqabi, G., G. Euler, D. Wiens, M. Wysession, S. van der Lee, J. Revenaugh, A. Frederiksen, F. Darbyshire, S. Stein, and D. Jurdy (2013). Array analysis of Lake Superior microseisms, *Abstract: 2013 EarthScope National Meeting*, Raleigh, North Carolina, 13–15 May 2013.

Anderson, K., R. Butler, and R. Aster (2008). Comparison of Antarctic seismic station quality performance to aggregate GSN network power spectral density probability density functions, *Annual Meeting of the Seismological Society of America, Santa Fe, New Mexico*, Santa Fe, New Mexico, 16–18 April 2008, *Seismol. Res. Lett.* 79, no. 2.

Anthony, R. E., R. C. Aster, D. A. Wiens, A. Nyblade, and C. A. Rowe (2011). Seismic noise levels across Antarctica, *AGU Fall Meeting Abstracts 2204*, San Francisco, California, 5–9 December 2011.

Ardhuin, F., E. Stutzmann, M. Schimmel, and A. Mangeney (2011). Ocean wave sources of seismic noise, *J. Geophys. Res.* **116,** C05002, doi: 10.1029/2011JC006952.

Aster, R. C., D. E. McNamara, and P. D. Bromirski (2008). Multidecadal climate-induced variability in microseisms, *Seismol. Res. Lett.* **79,** 194–202.

Aster, R. C., D. E. McNamara, and P. D. Bromirski (2010). Global trends in extremal microseism intensity, *Geophys. Res. Lett.* **37,** L14303, doi: 10.1029/2010GL043472.

Bromirski, P. D., F. K. Duennebier, and R. A. Stephen (2005). Mid-ocean microseisms, *Geochem. Geophys. Geosyst.* **6,** Q04009, doi: 10.1029/2004GC000768.

Butler, R., T. Lay, K. Creager, P. Earl, K. Fischer, J. Gaherty, G. Laske, B. Leith, J. Park, M. Ritzwoller, J. Tromp, and L. Wen (2004). The global seismographic network surpasses its design goal, *Eos Trans. AGU* **85,** no. 23, 225–229, doi: 10.1029/2004EO230001.

Chaput, J., R. Aster, X. Sun, D. Wiens, A. Nyblade, S. Anandakrishnan, A. Huerta, P. Winberry, and T. Wilson (2014). Crustal thickness across West Antarctica, *J. Geophys. Res.* **119,** 378–395.

Fetterer, F., K. Knowles, W. Meier, and M. Savoic (2002). *Sea Ice Index*, Digital media, Natl. Snow and Ice Data Center, Boulder, Colorado.

Galperin, E. I., I. L. Nersesov, and R. M. Galperina (1986). *Borehole Seismology and the Study of the Seismic Regime of Large Industrial Centers*, Reidel, Dordrecht, Netherlands, 315 pp.

Gow, A. J. (1963). Age Hardening of snow at the South Pole, *J. Glaciol.* **4,** no. 35, 521–536.

Gow, A. J. (1975). Time-temperature dependence of sintering in perennial isothermal snowpacks, *International Association of Hydrological Sciences Publications* **114,** 25–41.

Grob, M., A. Maggi, and E. Stutzmann (2011). Observations of the seasonality of the Antarctic microseismic signal, and its association to sea ice variability, *Geophys. Res. Lett.* **38,** L11302, doi: 10.1029/2011GL047525.

Hansen, S. E., A. Nyblade, D. S. Heezel, D. A. Wiens, P. Shore, and M. Kanao (2010). Crustal structure of the Gamburtsev Mountains, East Antarctica, from *S*-wave receiver functions and Rayleigh wave phase velocities, *Earth Planet. Science Lett.* **300,** 395–401.

Hasselmann, K. (1963). A statistical analysis of the generation of microseisms, *Rev. Geophys.* **1,** no. 2, 177–210.

Heeszel, D. S., D. A. Wiens, A. A. Nyblade, S. E. Hansen, M. Kanao, M. An, and Y. Zhao (2013). Rayleigh wave constraints on the structure and tectonic history of the Gamburtsev Subglacial Mountains, East Antarctica, *J. Geophys. Res.* **118,** 2138–2153.

Intergovernmental Panel on Climate Change (IPCC) (2007). *Climate Change 2007: The Physical Science Basis. Contributions of the Working Group 1 to the Fourth Assessment Report of the Intergovernmental Panel on Climate Change*, Solomon, S., D. Qin, M. Manning, Z. Chen, M. Marquis, K. B. Averyt, M. Tignor, and H. L. Miller (Editors), Cambridge University Press, Cambridge, United Kingdom and New York, New York, U.S.A.

Koch, F. W., D. A. Wiens, G. G. Euler, A. A. Nyblade, S. Anandakrishnan, A. Huerta, T. J. Wilson, and R. C. Aster (2013). Tracking the effect of sea ice cover on microseismic noise using two seismic arrays in Antarctica, *Abstract Seismological Society of America Annual Meeting*, Salt Lake City, Utah , 17–19 April 2013.

Kohnen, H. (1974). The temperature dependence of seismic waves in ice, *J. Glaciol.* **13,** 144–147.

Li, T. M. C., J. F. Ferguson, E. Herrin, and H. B. Durham (1984). High-frequency seismic noise at Lajitas, Texas, *Bull. Seismol. Soc. Am.* **74,** 2015–2033.

Lloyd, A., A. Nyblade, D. Wiens, S. Hansen, M. Kanao, P. Shore, and D. Zhao (2013). Uppermantle seismic structure beneath the East Antarctic shield from body wave tomography: Implications for the origin of the Gamburtsev Subglacial Mountains, *Geochem. Geophys. Geosyst.* **14,** doi: 10.1002/ggge.20098.

Longuet-Higgins, M. S. (1950). A theory of the origin of microseisms, *Phil. Trans. Roy. Soc. A* **243,** 1–35.

Lough, A. C., D. A. Wiens, C. G. Barcheck, S. Anandakrishnan, R. C. Aster, D. D. Blankenship, A. D. Huerta, A. Nyblade, D. A. Young, and T. J. Wilson (2013). Seismic detection of an active subglacial magmatic complex in Marie Byrd Land, Antarctica, *Nat. Geosci.* **6,** 1031–1035.

MacAyeal, D., E. Okal, and R. Aster (2006). Transoceanic wave propagation links iceberg calving margins of Antarctica with storms in tropics and N. hemisphere, *Geophys. Res. Lett.* **33,** L17502, doi: 10.1029/2006GL027235.

McNamara, D., and R. Boaz (2011). PQLX: A seismic data quality control system description, applications, and users manual, *U.S. Geol. Surv. Open-File Rept. 2010-1292.*

McNamara, D., and R. Buland (2004). Ambient noise levels in the continental United States, *Bull. Seismol. Soc. Am.* **94,** 1517–1527.

Mayewski, P. A., M. P. Meredith, C. P. Summerhayes, J. Turner, A. Worby, P. J. Barrett, G. Casassa, N. A. N. Bertler, T. Bracegirdle, A. C. Naveira Garabato, D. Bromwich, H. Campbell, G. S. Hamilton, W. B. Lyons, K. A. Maasch, S. Aoki, C. Xiao, and Tas van Ommen (2009). State of the Antarctic and southern Ocean climate system, *Rev. Geophys.* **47,** RG1003, doi: 10.1029/2007RG000231.

Nyblade, A., J. Amundson, S. Hansen, E. Ivins, M. Lazzara, M. Nettles, C. Raymond, and L. Stearns (2012). A facility plan for polar seismic and geodetic science, *Joint IRIS/UNAVCO Workshop Report, IRIS Consortium*, http://www.iris.edu/hq/files/publications/other_workshops/docs/APOS_FINAL.pdf (last accessed March 2014).

Oppenheim, A. V., and R. Schafer (1975). *Digital Signal Processing*, Prentice-Hall, Englewood Cliffs, New Jersey.

Patterson, W. S. B. (1994). *The Physics of Glaciers*, Third Ed., Pergammon Press, New York.
Peng, Z., J. Walter, R. Aster, A. Nyblade, D. Wiens, and S. Anandakrishnan (2014). Dynamically triggered icequakes in Antarctica, *Nat. Geosci.* doi: 10.1038/NGEO2212.
Peterson, J. (1993). Observation and modeling of seismic background noise, *U.S. Geol Surv. Technical Rept. 93–322*.
Rhie, J., and B. Romanowicz (2004). Excitation of Earth's continuous free oscillations by atmosphere-ocean-seafloor coupling, *Nature* **431,** 552–556.
Ringler, A. T., and C. R. Hutt (2010). Self-noise models of seismic instruments, *Seismol. Res. Lett.* **81,** doi: 10.1785/gssrl.81.6.972.
Sorrells, G. G. (1971). A preliminary investigation into the relationship between long-period seismic noise and local fluctuations in the atmospheric pressure field, *Geophys. J. Roy. Astron. Soc.* **26,** nos. 1/4, 71–82.
Stutzmann, E., M. Schimmel, G. Patau, and A. Maggi (2009). Global climate imprint on seismic noise, *Geochem. Geophys. Geosyst.* **10,** Q11004, doi: 10.1029/2009GC002619.
Tanimoto, T. (2007). Excitation of microseisms, *J. Geophys. Res.* **34,** L05308, doi: 10.1029/2006GL029046.
Traer, J., P. Gerstoft, P. D. Bromirski, and P. M. Shearer (2012). Microseisms and hum from ocean surface gravity waves, *J. Geophys. Res.* **117,** B11307, doi: 10.1029/2012JB009550.
Tsai, V. C., and D. E. McNamara (2011). Quantifying the influence of sea ice on ocean microseism using observations from the Bering Sea, Alaska, *Geophys. Res. Lett.* **38,** L22502, doi: 10.1029/2011GL049791.
Van den Broeke, M. (2008). Depth and Density of the Antarctic Firn Layer, *Arctic, Antarctic, and Alpine Research* **40,** 432–438.
West, M. E., C. F. Larsen, M. Truffer, S. O'Neel, and L. LeBlanc (2010). Glacier Microseismicity, *Geology* **38,** 319–322, doi: 10.1130/G30606.1.
Wiens, D. A., S. Anandakrishnan, J. P. Winberry, and M. A. King (2008). Simultaneous teleseismic and geodetic observations of stick-slip motion of an Antarctic ice stream, *Nature* **453,** 770–775, doi: 10.1038/nature06990.
Wiens, D., D. Heeszel, X. Sun, A. Lloyd, A. Nyblade, S. Anandakrishnan, R. Aster, J. Chaput, A. Huerta, S. Hansen, and T. Wilson (2013). Lithospheric structure of Antarctica and implications for Geological and Cryospheric evolution, *Proc. IASPEI Meeting*, Gothenburg, Sweden, July 2013.
Wilson, D., J. Leon, R. Aster, J. Ni, J. Schlue, S. Grand, S. Semken, S. Baldridge, and W. Gao (2002). Broadband seismic background noise at temporary seismic stations observed on a regional scale in the southwestern United States, *Bull. Seismol. Soc. Am.* **92,** 3335–3341.
Winberry, J. P., S. Anandakrishnan, R. B. Alley, R. Bindschadler, and M. King (2009). Basal Mechanics of ice streams: Insights from stick-slip motion, *J. Geophys. Res. Earth Surf.* F01016, doi: 10.1029/2008JF001035.
Winberry, J. P., S. Anandakrishnan, D. A. Wiens, and R. B. Alley (2011). Dynamics of ice-stream stick-slip motion, *Earth Planet. Sci. Lett.* **305,** 283–289.
Withers, M., R. Aster, C. Young, and E. Chael (1996). High-frequency analysis of seismic background noise and signal-to-noise ratio near Datil, New Mexico, *Bull. Seismol. Soc. Am.* **86,** 1507–1515.
Young, C. J., E. P. Chael, M. M. Withers, and R. C. Aster (1996). A comparison of high frequency (≥ 1 Hz) surface and subsurface noise environment at three sites in the United States, *Bull. Seismol. Soc. Am.* **86,** 1516–1528.

Robert E. Anthony
Richard C. Aster
Department of Geosciences
Colorado State University
Fort Collins, Colorado 80523 U.S.A.
robert.anthony@colostate.edu

Douglas Wiens
Department of Earth and Planetary Sciences
Washington University in St. Louis
St. Louis, Missouri 63130 U.S.A.

Andrew Nyblade
Sridhar Anandakrishnan
Department of Geosciences
Pennsylvania State University
University Park, Pennsylvania 16802 U.S.A.

Audrey Huerta
J. Paul Winberry
Department of Geological Sciences
Central Washington University
Ellensburg, Washington 98926-7418 U.S.A.

Terry Wilson
Department of Geological Sciences
275 Mendenhall Lab
125 S. Oval Mall
Ohio State University
Columbus, Ohio 43210-1522 U.S.A.

Charlotte Rowe
EES-17, MS F-665 Seismologist
Geophysics Group
Los Alamos National Laboratory
Los Alamos, New Mexico 87545 U.S.A.

Published Online 26 November 2014